Optimization of Experimental Protocol in Order to Form SEBS Film via Dip-Coating the Copper Surface Using Response Surface Methodology

Fatma MASMOUDI and Mohamed MASMOUDI *

Posted Date: 26 May 2023

doi: 10.20944/preprints202305.1840.v1

Keywords: Coating; Copper; SEBS; Corrosion; Box-Behnken Design

Article

Optimization of Experimental Protocol in Order to form SEBS Film via Dip-Coating the Copper Surface Using Response Surface Methodology

Fatma Masmoud [1], Abdulrahman Mallah[2] and Mohamed Masmoudi [1,3,*]

[1] Laboratory of Electrochemistry and Environment (LEE), Sfax National Engineering School (ENIS) BPW, University of Sfax, Sfax 3038, Tunisia
[2] Department of Chemistry, College of Science, Qassim University, P.O. Box 6644, Buraydah Almolaydah, Buraydah 51452, Saudi Arabia
[3] Preparatory Institute for Engineering Studies of Sfax, BP 805, 3018, University of Sfax, Tunisia
* Correspondence: med_mmasmoudi@yahoo.fr

Abstract: Organic Coatings have potential applications in the prevention of metal corrosion in an aqueous solution. The protective effect of SEBS coated copper corrosion in NaCl 3% solution was investigated by using electrochemical methods. The main objective of this work is to find the optimal conditions of the protocol immersion to evaluate the effects of SEBS ratio and two-immersion time on the anticorrosive behaviour of copper in 3 wt % NaCl solution in order to determine the best conditions to produce a protective SEBS film on the copper surface. Response Surface Methodology (RSM) is used as an optimization method. The study's findings show the combination of three environmental factors that minimize corrosion rate. The Box-Behnken Design (BBD) is working perfectly for the statistical significance of the model (ANOVA test). This analysis calculates the contribution value of each parameter in changing the value of the corrosion rate (CR) in not only individual but also synergistic cases. The optimized parameters were found to be a 2.17% of SEBS ratio, 20 min of immersion 1, and 21 min of immersion 2. The electrochemical impedance spectroscopy tests confirmed the results.

Keywords: coating; copper; SEBS; corrosion; Box-Behnken Design

1. Introduction

It is difficult for a single material to meet various demands such as excellent electrical conductivity, better thermal properties and high strength with the rapid development of the manufacturing industry [1,2]. Copper is one of the widely used electronic and energy materials. This metal is a fairly precious. Yet, it can be severely corroded in the presence of aggressive ions such as chloride, which significantly restricts its use [3]. In order to protect the copper from being corroded, different strategies can be used. Among the different techniques, surface coating on copper provides an economical means to tackle the corrosion problem. Adding polymeric coatings is an efficient way to protect metals from corrosive conditions. Research used natural and synthetic polymers to protect metals from corrosion instead of toxic inorganic and organic corrosion inhibitors.

Recently, thermoplastic elastomers (TPEs) have become commercially important materials because of their excellent chemical resistance and desirable physical properties equivalent to vulcanized rubbers [4]. Polystyrene-block-poly (ethylene-ran-butylene)-block-polystyrene) (SEBS) is a triblock styrene copolymer. It is extensively used thermoplastic elastomer [5]. SEBS is characterized by their elasticity, versatility in processing, thermo-plasticity, thermo-oxidative stability, ultraviolet resistance, high service temperature, good low-temperature properties design, recyclability, manufacturing it at lower cost. These various SEBS characteristics are exploited in several areas such as conductive adhesives, electromagnetic shielding materials and anti-corrosive coatings [6–9].

In our previous study, the SEBS was successfully deposited on the copper surface with a defined immersion protocol [10]. The protective effect of SEBS coated on copper corrosion in NaCl 3% solution, as well as the effect of SEBS ratio in the resistance corrosion was investigated by using

 doi:10.20944/preprints202305.1840.v1

electrochemical methods. The potentiodynamic polarization and electrochemical impedance spectroscopy findings reveal that the SEBS copolymer coatings considerably suppress the corrosion current density, increase the charge transfer resistance and effectively inhibit corrosion of the copper. Our previous study was consecrated only the effect of the SEBS ratio on the electrochemical behaviour of SEBS coated copper. Moreover, the immersion protocol can depend on other factors. Eexperimental design should be used to determine the variables that significantly influence the CR of Cu-SEBS.

In this study, the RSM was employed as an optimization method while the Statgraphics software was used to treat experimental design data. RSM represents a set of mathematical and statistical techniques that are valuable for formulating experiments, developing models, and evaluating the impact of numerous independent variables [11]. The main advantage of this method is not only to ensure greater reproducibility and quality but also to decrease the cost, reduce the number of experiments required and the consideration of interactions among the variables. This method is also used to optimize the operating parameters in multivariable systems [12,13]. Nowadays, the chemometric approach is considered a powerful tool for studying the corrosion and protection process. We—along with some authors—have introduced the use of the experimental design to understand metals corrosion and inhibition [14–18]. The RSM is an efficient procedure in making an approximation and optimization of the stochastic models [19]. Among the common RSMs used in optimization process are Doehlert Design (DD), Central Composite Design (CCD) and Box-Behnken Design (BBD). The BBD is much more efficient than CCD by 11.5%, which means the former requires fewer experimental runs than the latter. The advantages of RSM need less effort, expense, and time derived from fewer experiments while providing all the necessary information to design a process of interest [19]. For example, to monitor four variables at four different levels, the BBD of the experiment entails just 29 experimental runs, including the 5 center points. However, a full four-level factorial design needs 256 experimental runs.

Considering the above-mentioned aspects, the key objectives of our research are as follows:

(i) highlighting the use of experimental design and RSM to assess the impacts of the basic operating parameters (SEBS ratio, immersion 1 and immersion 2) in the process of the treatment of the SEBS coated copper (Cu-SEBS) on the response factor (CR),

(ii) determining, modelling, and optimizing the best conditions to produce SEBS coating on the copper which presents the lowest value of corrosion rate and

(iii) verifying the model built by experimental design and RSM by using these optimal operating parameters to explore the corrosion behaviour of the SEBS coated copper at optimal conditions (Cu-SEBS-Opt-Cond) in a 3 wt% NaCl solution.

2. Experimental

2.1. Pre-treatment of copper electrodes

The specimens were made from copper having a purity of 99.9%. The area of the copper electrode exposed to the electrolyte was 1 cm^2. Surface pre-treatment of the specimens was performed by polishing the surface with successive grades of SiC paper from 240 to 1000 grade. These copper electrodes were cleaned with ultra-pure water and finally dried.

2.2. Preparation of SEBS coated copper electrodes

SEBS solution was prepared by dissolving different SEBS ratio in toluene solvent. Then we stirred the mixture for 60 min at a room temperature (about 25° C). To form Cu-SEBS, we have applied a defined immersion protocol. This latter consists of the pre-treated specimens' immersion in SEBS solution for different time: immersion 1. After this, the obtained coatings were first dried at 25 °C for 10 min then for 20 min in an oven at 80°C. In the next stage, the re-immersion of these pre-treated specimens in SEBS solution was made for different time: immersion 2. Finally, the coatings we get were dried at 25 °C for 10 min.

For each electrochemical corrosion test, this procedure was repeated.

 doi:10.20944/preprints202305.1840.v1

Preprints (www.preprints.org) | NOT PEER-REVIEWED | Posted: 26 May 2023 doi:10.20944/preprints202305.1840.v1

2.3. Experimental design

In this work, we optimized the three independent variables using the RSM which is called Box Behnken Design (BBD) to find the optimal condition of protocol immersion realized the minimum corrosion rate of Cu-SEBS electrodes with a few experiments and analyse the independent variables' interaction. SEBS ratio (in % mass with respect to total mass of the solution SEBS-Toluene), immersion 1 (min), and immersion 2 (min) were input as independent variables. The CR of Cu-SEBS in aqueous NaCl environment was the response factor. The independent variables of the CR and their respective ranges are mentioned in Table 1.

Table 1. Coded levels of operating variables.

Factor	Symbols	Levels		
		Low (-1)	Centre (0)	High (+1)
SEBS ratio (%)	A	1.1	2	2.9
Immersion 1 (min)	B	10	20	30
Immersion 2 (min)	C	30	20	30

Equation (1) allows us to obtain the number of experiments (N) required for BBD:

$$N = 2k\,(k\text{-}1) + Cp \quad (1)$$

where k and Cp represent the number of factors and replicate number of central point respectively. A total of 15 experiments have been carried out for three independent factors—each at three levels—to study the effects of factors on the CR.

To determine the coefficients in the response model, the measured data were fitted into second order polynomial equation. A second order polynomial equation where all the linear, square and interaction terms have been incorporated can be expressed as the Equation (2):

$$Y = \beta_0 + \sum_{i=1}^{n} \beta_i \chi_i + \sum_{i=1}^{n} \beta_{ii} \chi_i^2 + \sum_{i=1}^{n-1} \sum_{\substack{j=2 \\ j>1}}^{n} \beta_{ij} \chi_i \chi_j + \varepsilon \quad (2)$$

Y represents the predicted response. β_0, β_i, β_{ii} and β_{ij} are constant, linear, quadratic and interaction coefficients of the model. X_i and X_j are the coded independent factors. ε represents the error of the model.

In this study, we use the Statgraphics software XVIII to analyse the data and calculate the predicted responses of experimental design. The validity of the model was ascertained by using analysis of variance (ANOVA).

2.4. Electrochemical studies

Cu-SEBS was analysed at room temperature by electrochemical techniques using a Potentiostat / Galvanostat radiometer controlled using the VoltaLab software for which an electrochemical cell was built with a Saturated Calomel Electrode as reference electrode, a platinum bar as auxiliary electrode, copper as working electrode and an aqueous solution of NaCl 3 % as electrolyte prepared using distilled water.

2.4.1. Potentiodynamic polarization studies

The potentiodynamic polarization measurements were carried out in the potential range from −400 to + 600 mV with a scanning rate of 0.5 mV s^{-1}.

2.4.2. Voltammetry around OCP (ΔE=± 50 mV)

The voltammetry around open circuit potential (OCP) measurements was obtained on a restricted scale of capability around OCP to engender just a small perturbation of the metal surface. The potential was moved from the OCP to OCP + 50 mV, then down to OCP −50 mV and back to

Preprints (www.preprints.org) | NOT PEER-REVIEWED | Posted: 26 May 2023 doi:10.20944/preprints202305.1840.v1

OCP, at a scan rate equal to 0.5 mV s^{-1}. The data of the voltammetry around OCP measurements were fitted to the Tafel equation, using EC-Lab V10.32 software (Bio-Logic) to estimate the corrosion current density (j_{corr}), Tafel coefficients (β_a and β_c) and corrosion rate (CR).

2.4.3. Electrochemical impedance studies

Impedance studies of bare copper and Cu-SEBS were conducted in aqueous NaCl solution. The electrode potential was stabilized after 30 min. These studies were performed in the frequency range from 100 kHz to 5 mHz under excitation of a sinusoidal wave of 10 mV amplitude. The impedance spectra were fitted using electrical equivalent circuits with EC-Lab software.

3. Results and discussion

3.1. Statistical treatment of data

The response factor is CR of Cu-SEBS in an aqueous NaCl environment, obtained from voltammetry around OCP (ΔE = ± 50 mV vs SCE). In order to stabilize the OCP, prior to every experiment, we immerse the electrodes in the solution for half an hour.

As it is mentioned in Figure 1, the obtained examples of comparison between the experimental polarization curve and Tafel simulated curve with EC-Lab software for experiment 1 (-1,-1,0), experiment 2 (1,-1,0) and experiment 13 (0,0,0) after a 30-min exposure in 3 wt% NaCl aqueous solution.

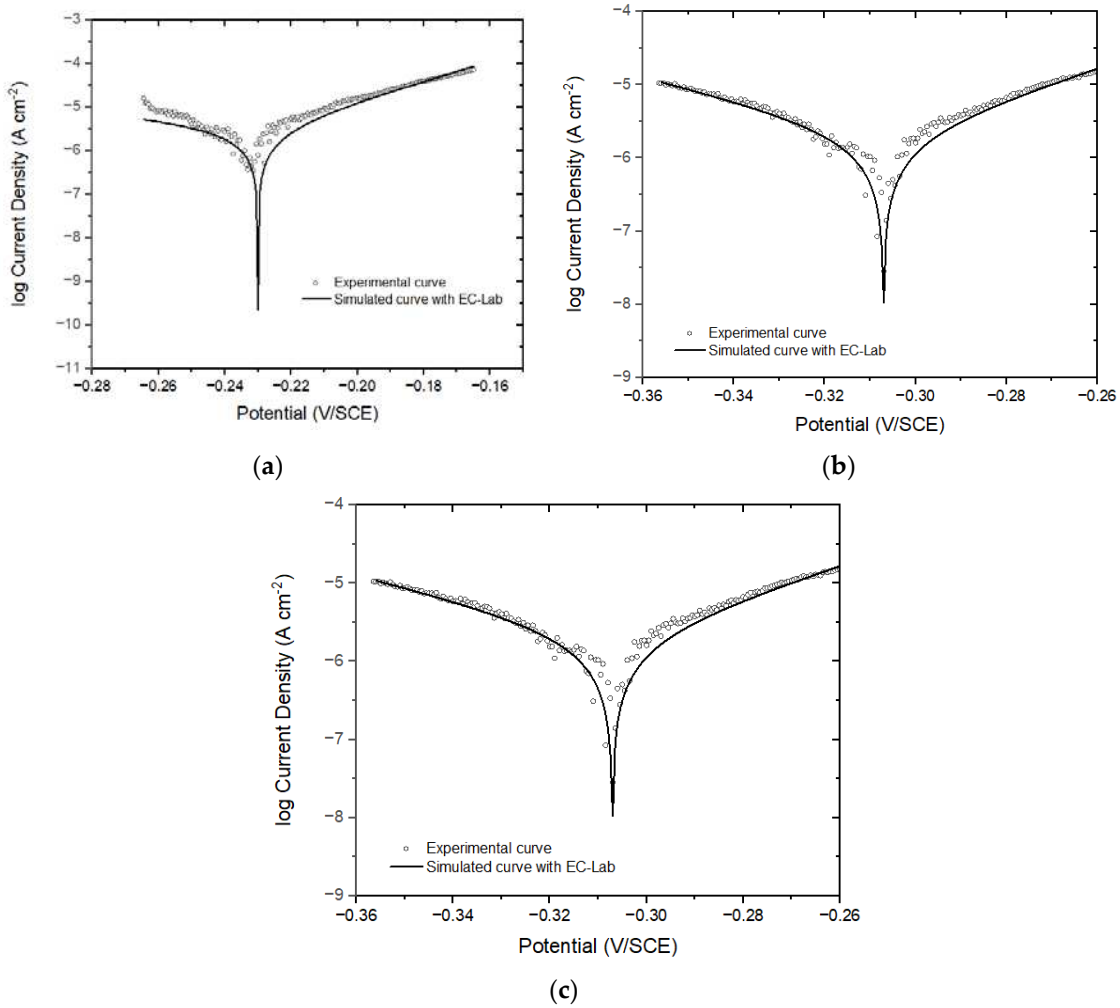

Figure 1. Tafel curves simulated with EC-Lab of (a) Experience 1 (b) Experience 2 and (c) Experience 13 after exposure in a 3 wt% NaCl solution for 30 min compared to experimental polarization curve around OCP.

Preprints (www.preprints.org) | NOT PEER-REVIEWED | Posted: 26 May 2023 doi:10.20944/preprints202305.1840.v1

The obtained CR values (responses) from the experiments suggested by the Box-Behnken design were fitted to linear, interactive and quadratic models in order to find the regression equations.

We selected the quadratic model because it has a low standard deviation (0.07), high values of R^2 (0.9461) and adjusted R^2 (0.8491).

The multi-regression analysis of experimental data allowed us to find the empirical relationship between the CR and independent variables which can be calculated by the second-order polynomial expression in terms of paramount actual factors as:

$$\mathbf{CR} = 0.24135 - 0.11008\,A - 0.00222\,B - 0.00718\,C + 0.01412\,A^2 + 0.00068AB +$$

$$0.00112AC - 0.000024\,A^2 + 0.000055\,BC + 0.000073\,C^2$$

where: A is the SEBS ratio; B is the immersion 1; C is the immersion 2; A^2 is the quadratic effect of SEBS ratio; C2 is the quadratic effect of immersion 2; AB is the interaction between SEBS and immersion 1; AC is the interaction between SEBS and immersion 2.

The adjusted R^2 is 0.9461—within the acceptable limits of $R^2 \geq 0.80$- revealing an excellent fitting of the experimental data with the second-order polynomial equation.

The impact of the immersion protocol factors on CR is shown in Figure 2.

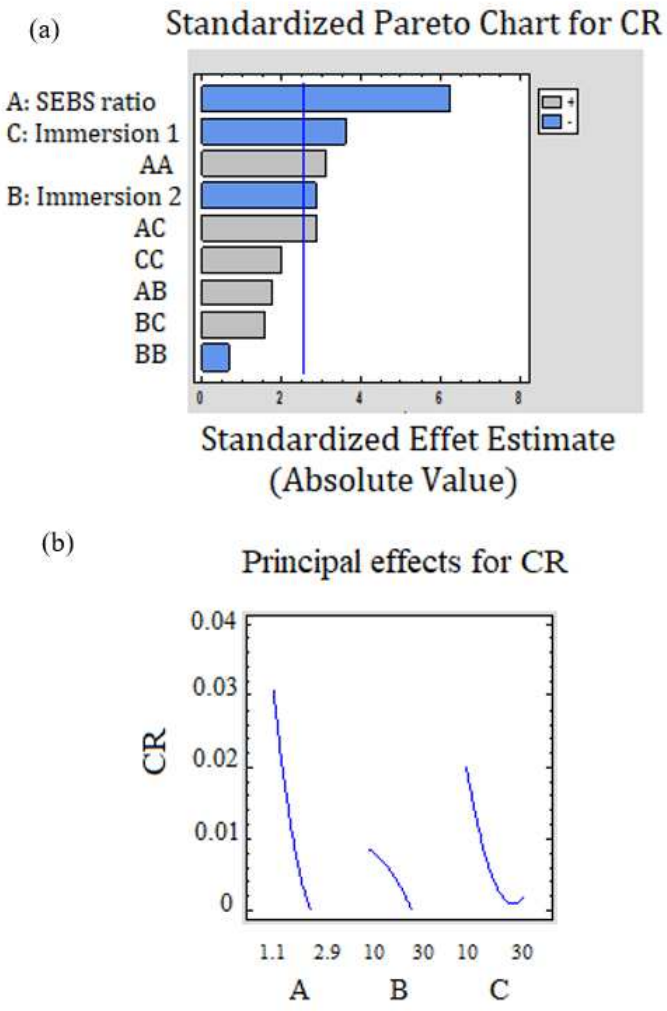

Figure 2. Effect of immersion protocol factors on corrosion rate; a: Standardized Pareto chart; b: main effects for CR. A: SEBS ratio; B: Immersion 1; C: Immersion 2.

Pareto chart shows ANOVA (values' analysis) for operating parameters and their combinations reveal their own impacts from the most important level to the least one at 5%. The vertical line points to this statistical level.

Preprints (www.preprints.org) | NOT PEER-REVIEWED | Posted: 26 May 2023 doi:10.20944/preprints202305.1840.v1

Figure 2a reveals that three parameters have a significant effect on the CR. The impacts of SEBS ratio (A), immersion 1 (B), and immersion 2 (C) are negative. It means the higher these parameters are, the lower the CR is. The positive values of the quadratic effect of SEBS ratio (A^2) reflects a CR evolution but at a minimal level. In fact, it should be pointed out that the interaction between SEBS and immersion 2 (AC) and the quadratic effect of immersion 2 (C^2) are not beneficial for reducing the CR.

The experimental design findings in Figure 2b reveal the impacts of every parameter (SEBS ratio, immersion 1 and immersion 2) on CR separately. Figure 2b shows that the higher the SEBS ratio' level is, the lower the CR is. We have noticed the same trends for the immersion 1 and the immersion 2 factors. However, evolution of SEBS ratio factor is more remarkable (slope SEBS ratio is more significant). This discovery means that the bases of the CR could be obtained with a high SEBS rate and a high immersion 2.

3.2. Response surfaces for Corrosion Rate CR

The three-dimensional plots (Figure 3) reveal the single effects of the process variables and how they interacted on CR. We obtained the surfaces observed by plotting the CR's measured values against only two factors while keeping the third factor's level in the middle.

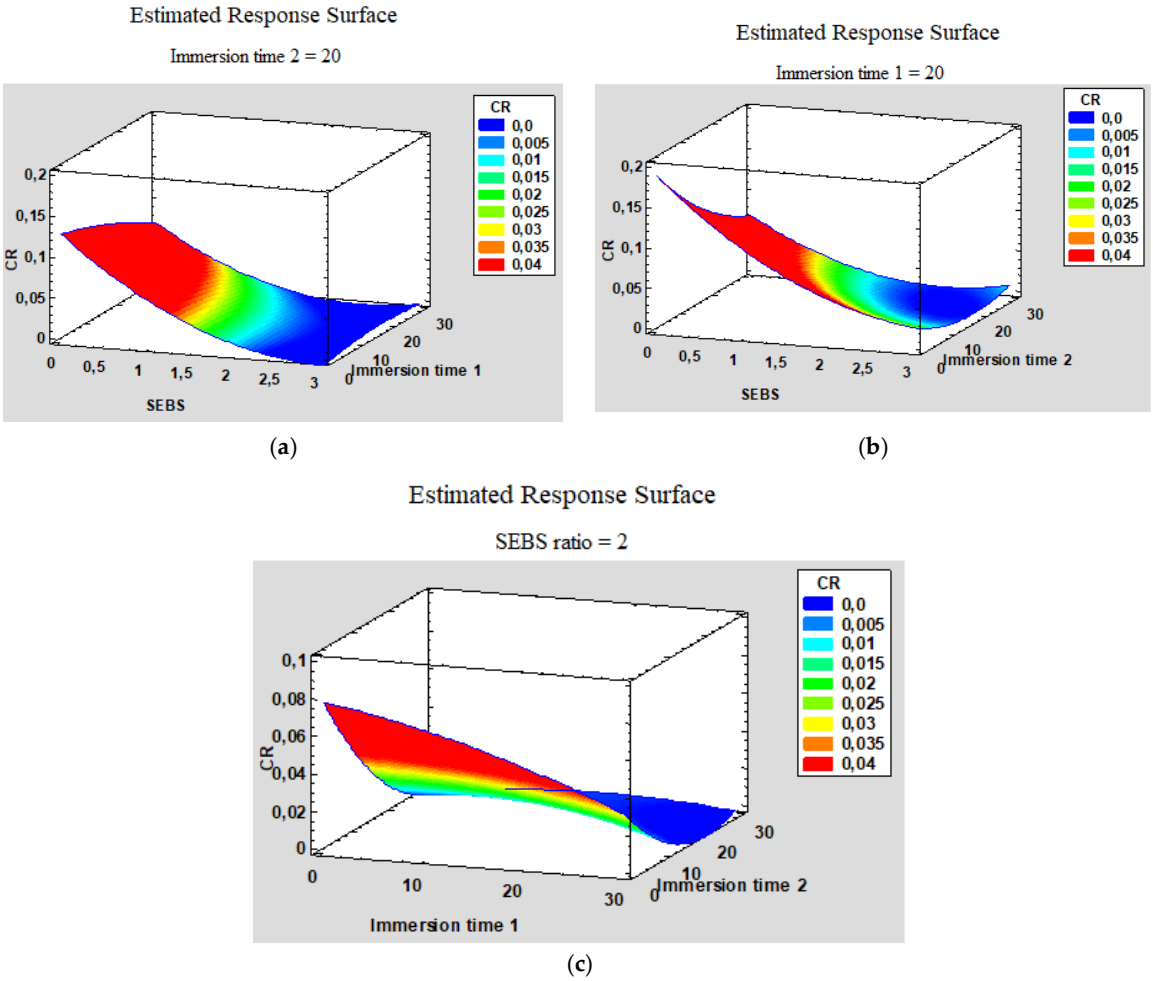

Figure 3. Response surfaces for CR (**a**) SEBS and immersion 1 at 20 min of immersion 2, (**b**) SEBS and immersion 2 at 20 min of immersion 1, (**c**) of immersion 1 and of immersion 2 at 2% of SEBS.

As it is shown in Figure 3a, CR dropped sharply with A whatever the value of B is. Reciprocally, the same plot reveals that there is a considerable decline in CR with B if A is low, whereas it shows no significant change with B if A is high. Taking into consideration the influence of both A and C, Figure 3b shows that CR decreases sharply with A if C is low while it decreases considerably with A

Preprints (www.preprints.org) | NOT PEER-REVIEWED | Posted: 26 May 2023 doi:10.20944/preprints202305.1840.v1

until becomes constant if C is high. Reciprocally, the same plot reveals that CR decreases significantly with C if A is low, and it shows declines considerably with C until minimum if A is high. Lastly, Figure 3c shows that CR declines when B and C values increase despite the fairly limited variations.

The shape of the—more or less distorted—response surface is an excellent indication showing the interactive effects between variables. Consequently, Figure 3b shows a strong interaction between the SEBS ratio and immersion 2 (AC). In contrast, Figure 3a,c show little interaction effects between the SEBS ratio and immersion 1 (AB) and immersion 1 and immersion 2 (BC) respectively because the response surfaces of these figures do not have a twisted aspect too.

Figure 4 plots the response surface model's contour diagram as function of SEBS ratio and immersion 2 with immersion 1 is constant at 20 min.

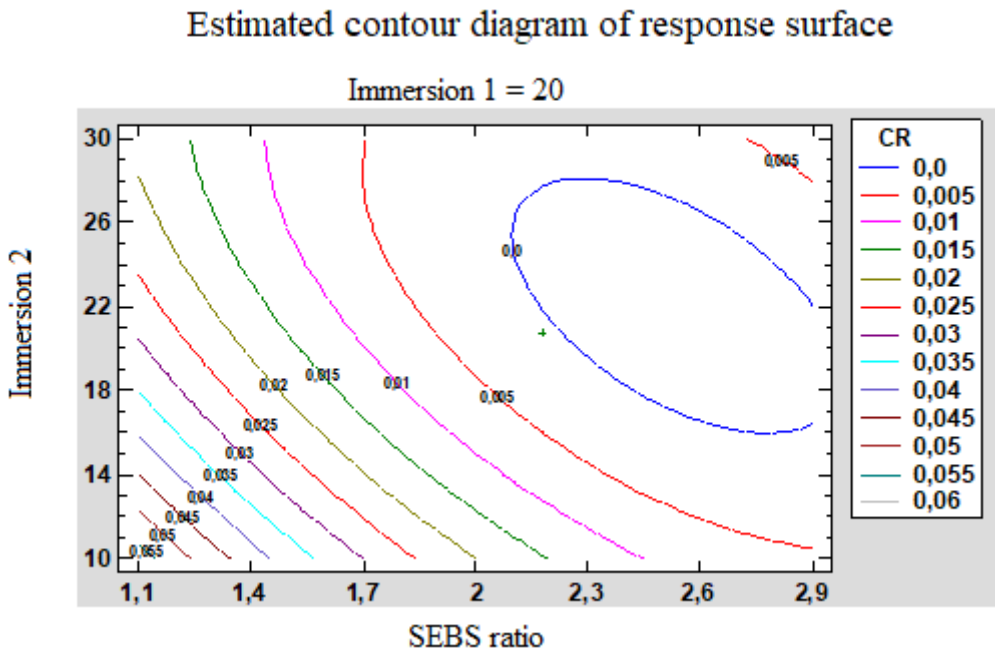

Figure 4. Contour diagram of response surface model of the corrosion rate as the function of SEBS ratio and immersion 2 with immersion 1 is constant at 20 min.

It can be shown that low CR values are obtained when SEBS ratio is greater than 2%.

These results reveal that the use of the higher SEBS ratio is desirable for obtaining a low corrosion rate, and the immersion time 1 and 2 do not need to be high.

3.3. Optimal operating conditions experiment

After studying the independent variables' impact on the response, we identify that the optimum values of operating parameters generate the minimum corrosion rate by not only solving the quadratic regression model but also analyzing the response surface contour plots. The fit for this experimental design determined using Statgraphics software's model enabled us to find the three optimal values of the operating parameters, SEBS ratio (A), immersion 1 (B) and immersion 2 (C) in the studied ranges (Table 1).

The optimum process conditions for A, B and C that we reached were 2.17%, 20 min and 21 min respectively. Under these conditions, we found the CR predicted by the model was 0,0001 mm/year.

To confirm these results we have studied the electrochemical behaviour of the SEBS coating copper under optimal conditions of immersion protocol (Cu-SEBS-Opt-Cond) exposed in 3% NaCl solution while using the techniques of potentiodynamic polarization and electrochemical impedance spectroscopy (EIS).

Preprints (www.preprints.org) | NOT PEER-REVIEWED | Posted: 26 May 2023 doi:10.20944/preprints202305.1840.v1

3.3. Confirmation of the results by electrochemicalstudies

3.3.1. Potentiodynamic polarization studies

3.3.1.1. Potentiodynamic polarization between -0.4 and +0.6 V vs SCE

We list in Figure 5 the potentiodynamic polarization curves for bare copper and SEBS-coated copper at best operating conditions (Cu-SEBS-Opt-Cond) in a naturally aerated 3 wt% NaCl solution at 25 °C.

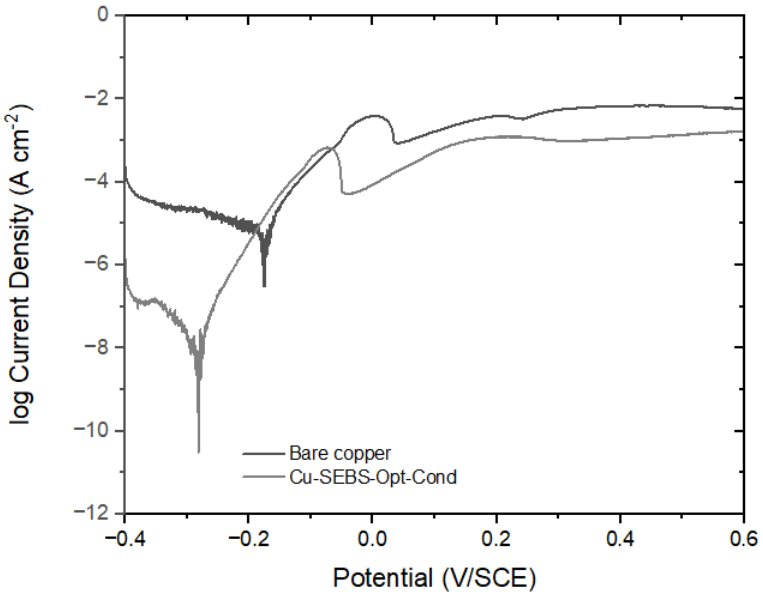

Figure 5. Potantiodaynamic polarization curves of Bare Copper and Cu-SEBS-Opt-Cond obtained after 30 min immersion in 3 wt% NaCl solution at RT (~25 °C).

As mentioned in our previous works, the bare copper has three chief regions of potential in the anodic part [10,20,21]. In fact, the first region is identified by the oxidation of copper (Equation (3)).

$$Cu \rightarrow Cu^{+} + e^{-} \quad (3)$$

The second region emanates from the formation of into an insoluble film CuCl $_{(film)}$ (Equation (4)).

$$Cu^{+} + Cl^{-} \rightarrow CuCl_{(film)} \quad (4)$$

The third region is characterized by the the soluble cuprous complex $CuCl_2^-$ (Equation (5)).

$$CuCl + Cl^{-} \rightarrow CuCl_2^{-}{}_{(surface)} \quad (5)$$

The oxygen reduction reaction is the major cathodic reaction that influences the corrosion processes (Equation 6).

$$O_2 + 2H_2O + 4e^{-} \leftrightarrow 4OH^{-} \quad (6)$$

For the Cu-SEBS-Opt-Cond electrode, it is evident that the CEBS's formation on the copper surface controlled the cathodic O_2 reduction processes, while there is no effect on the anodic metal dissolution. Additionally, the cathodic curve produces a roughly parallel line, indicating the cathodic mechanism (the oxygen reduction) does not change. Moreover, the electric current density decreases from 1.584 10^{-4} A cm^{-2} for bare copper to 6.309 10^{-7} A cm^{-2} for Cu-SEBS-Opt-Cond. In addition, the corrosion potential (E_{corr}) shifts to the cathodic side. These results are in accordance with our previous study's finding that SEBS is a cathodic-type inhibitor [10].

Preprints (www.preprints.org) | NOT PEER-REVIEWED | Posted: 26 May 2023 doi:10.20944/preprints202305.1840.v1

3.3.1.2. Voltammetry around OCP (ΔE = ± 50 mV vs SCE)

Figure 6 exhibits the results of voltammetry around OCP (ΔE = ± 50 mV vs SCE) of bare copper and Cu-SEBS-Opt-Cond obtained after 30-min immersion in 3 wt % NaCl solution.

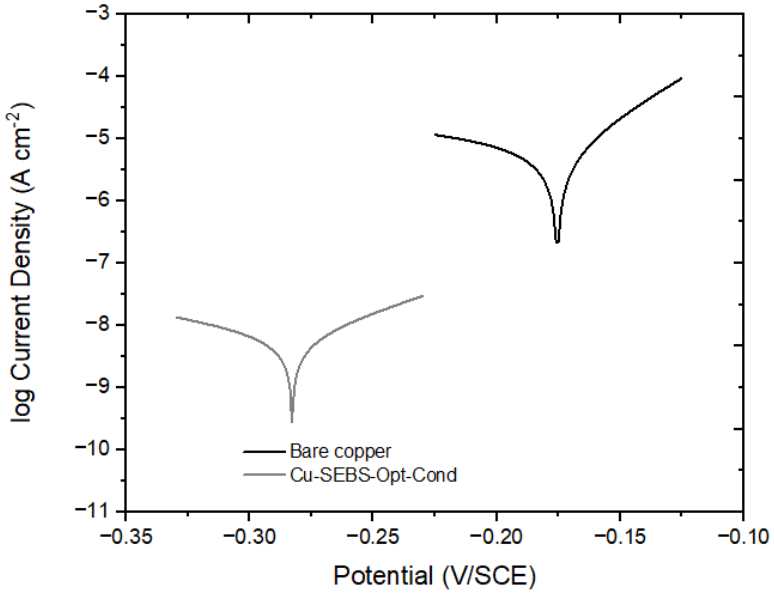

Figure 6. Polarization curve around OCP of of Bare Copper and Cu-SEBS-Opt-Cond obtained after 30 min immersion in 3 wt% NaCl solution at RT (~25 °C).

We list the electrochemical parameters extracted from this figure and simulated with EC-Lab software in Table 2.

Table 2. Electrochemical kinetic parameters obtained from the curves polarization around OCP and simulated with EC-Lab software for Bare Copper and Cu-SEBS-Opt-Cond in 3wt% NaCl solution at RT (~25 °C).

Electrode	E_{corr} (mV/SCE)	j_{corr} μA cm^{-2}	CR ×10^{-3} mm year^{-1}	η (%)
Bare Copper	-175	6.83	79.24	–
Cu-SEBS-Opt-Cond	-282	0.015	0.174	99.7

The corrosion density, j_{corr}, which is directly related to the corrosion rate, decreased sharply after SEBS coating on copper at optimal conditions of immersion protocol. j_{corr} for Cu-SEBS-Opt-Cond equal 0.015 μA cm^{-2} and CR equal 0.000174 mm year^{-1}. This value is close to that found by the experimental design (0.0001 mm year^{-1}).

Furthermore, the protective action of the SEBS coating is explained by the decline of j_{corr}. It can be quantified through the protection efficiency (η) and calculated according to the following Equation (7) [22]:

$$\eta = \frac{j^0_{corr} - j_{corr}}{j^0_{cor}} \times 100 \quad (7)$$

where j^0_{corr} and j_{corr} are the corrosion current densities of the bare copper and Cu-SEBS-Opt-Cond, respectively.

The Cu-SEBS-Opt-Cond's protection efficiency (η) equals 99.7%. This value is high enough to prove the ability of SEBS which is formed on the copper surface to inhibit the corrosion of copper in chloride media.

Preprints (www.preprints.org) | NOT PEER-REVIEWED | Posted: 26 May 2023 doi:10.20944/preprints202305.1840.v1

3.3.2. Electrochemical impedance spectroscopy (EIS)

Figure 7 represents the Nyquist diagram of bare copper obtained after a 30-min immersion in 3 wt % NaCl solution at 25 °C.

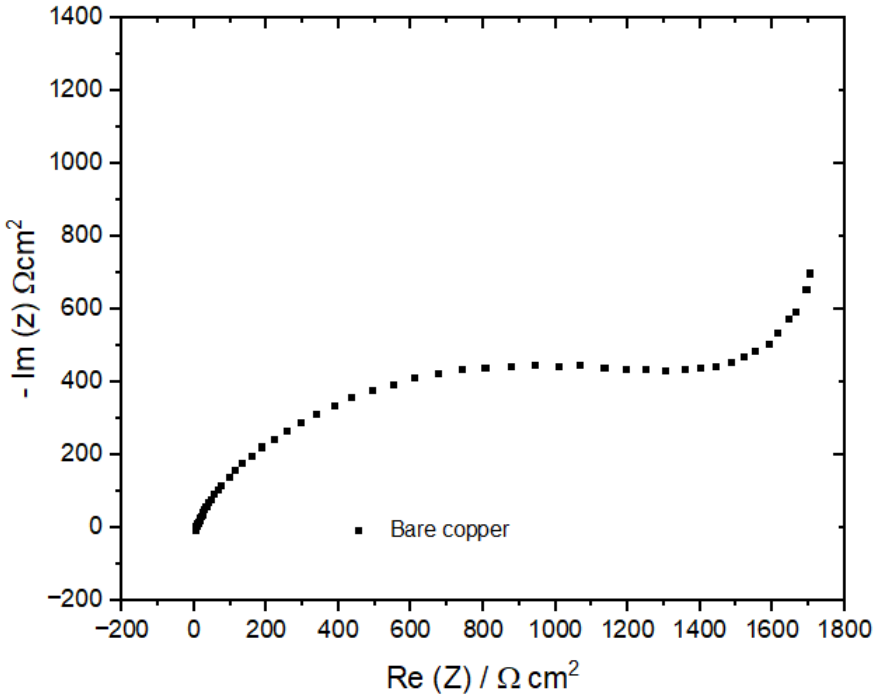

Figure 7. Nyquist plots for Bare Copper obtained after 30 min immersion in 3 wt% NaCl solution at RT (~25 °C).

The diagram mainly reveals a capacitive loop at high frequency and an almost linear curve, making a 45°angle with the Re (Z) axis at low frequency [10,21–23]. The semicircle in the high-frequency region shows the combination of double-layer capacitance and charge-transfer resistance. Moreover, the semi-circle's depression can be attributed to the frequency dispersion resulting from the roughness and inhomogeneity of the electrode surface [21,24,25]. Furthermore, the Warburg impedance's presence in the low-frequency region is related to the anodic diffusion process of copper species ($CuCl_2^-$). These species are soluble within the copper surface towards the saline solution. The Warburg's presence is also associated with the cathodic diffusion process of the oxygen's dissolution within the saline solution towards the electrode surface.

Figure 8 indicates the Nyquist plots of bare copper and Cu-SEBS-Opt-Cond obtained after a 30-minute immersion in an aqueous 3 wt% NaCl solution.

Preprints (www.preprints.org) | NOT PEER-REVIEWED | Posted: 26 May 2023 doi:10.20944/preprints202305.1840.v1

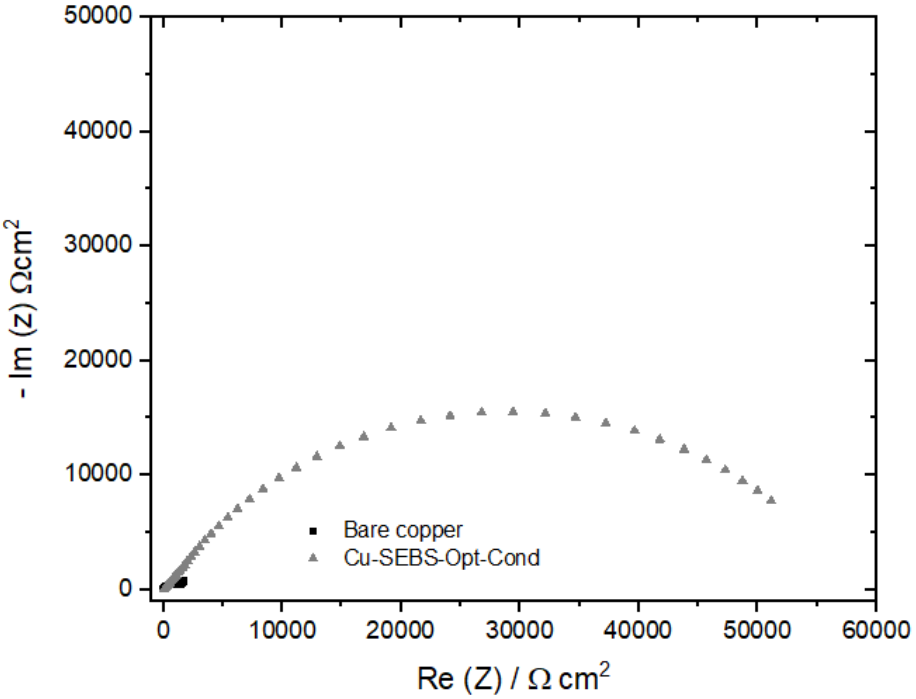

Figure 8. Nyquist plots for Bare Copper and Cu-SEBS-Opt-Cond obtained after 30 min immersion in 3 wt% NaCl solution at RT (~25 °C).

In the presence of SEBS coating at optimal conditions, the diagram's diameter strongly increases, confirming the clearly observed inhibiting effect by means of voltammetry. In addition, the Warburg impedance disappearance indicates that the film is sufficiently densely-packed to prevent the oxygen or Cl^- ions' diffusion to the copper substrate, thus inhibiting the copper corrosion [26].

We obtained more accurate information through the impedance data's analysis with electrical equivalent circuits (EEC). We display the two considered EEC in Figure 9.

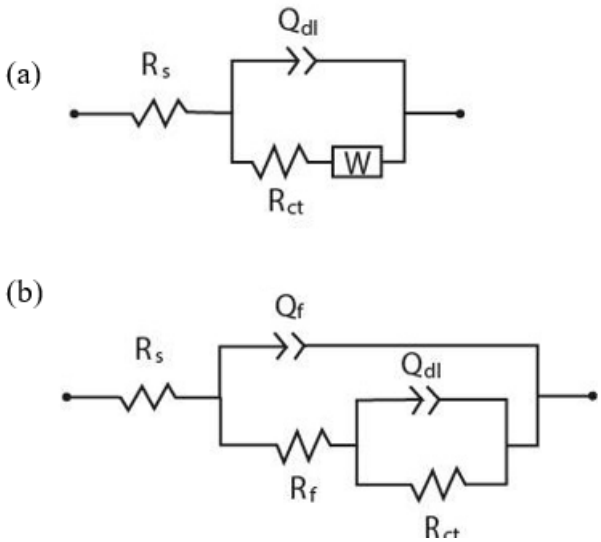

Figure 9. Equivalent circuits (**a**) Equivalent circuits $R_s(Q_{dl}(R_{ct}W))$ (**b**) $R_s(Q_f(R_f(Q_{dl}R_{ct})))$ used to fit the EIS experimental data.

In these circuits, R_s is the solution resistance, R_{ct} is the charge transfer resistance, Q_{dl} corresponds to the capacitance of the double layer, R_f and Q_f are associated with the film of corrosion products which was formed on the metal surface and W is the Warburg impedance linked to the diffusion processes in the low frequency region.

Preprints (www.preprints.org) | NOT PEER-REVIEWED | Posted: 26 May 2023 doi:10.20944/preprints202305.1840.v1

In fact, Q_{dl} and Q_f are constant phase elements (CPE) used in place of capacitors to compensate for deviations from ideal dielectric behavior that are due to the heterogeneous nature of the electrode surface. We have listed the obtained findings after the computer fitting of the experimental impedance data in Table 3. The parameter n describes how electrode departs from an ideal surface, corresponding to n = 1 (and the CPE, to an ideal capacitor). n_f and n_{dl} are associated with Q_f and Q_{dl} in Table 3, respectively.

The CPE's impedance function is described according to Equation (8):

$$Z_{CPE} = {}^{1}/_{Q_0 (j\omega)^n} \quad (8)$$

where Q_0 represents the CPE magnitude, j is the imaginary root, ω is the angular frequency, and n is the exponential term that can be used as a measure of the inhomogeneity or roughness of the electrode surface. n denotes the shift phase and its value ranges from 0 to 1. The smaller the n value becomes, the rougher the surface as well as the more serious the corrosion [10].

Table 3. Electrochemical impedance parameters for Bare Copper and Cu-SEBS-Opt-Cond in 3 wt% NaCl solution RT (~25 °C).

	Bare Copper	Cu-SEBS-Opt-Cond
-		
Rs (Ω cm²)	7.03	14.7
R_{ct} (Ω cm²)	1231	44457
$Q_{dl}.10^{-6}$(F cm^{-2} s_{dl}^n)	121	2.857
n_{dl}	0.711	0.885
R_f (Ω cm²)	–	13918
$Q_f.10^{-6}$(F cm^{-2} s_f^n)	–	28.61
n_f	–	0.611
W (Ω^{-1} cm^{-2} s$^{0.5}$)	190.8	–
η (%)	–	97.89

Table 3 reveals that the parameters, estimated for the bare copper accord well with the already published literature [27]. The charge transfer resistance (R_{ct}) value of the Cu-SEBS-Opt-Cond (44457 Ω cm²) is clearly more important than that of bare copper (1231 Ω cm²). Besides, the polarization resistance value, R_p, (R_p, is the sum of the R_{ct} and R_f) of Cu-SEBS-Opt-Cond equals 58375Ω cm² which is 47-fold higher than that of bare copper.

Table 3 also presents the protective efficiency (η) determined by the electrochemical impedance spectroscopy, which is calculated according to Equation (9) [28]:

$$\eta = \frac{R_p - R_p^0}{R_p} \times 100 \quad (9)$$

Both R_p^0 and R_p are the polarization resistance of bare copper and Cu-SEBS-Opt-Cond, respectively.

It was observed that η reached 97.89 % after coating the copper with SEBS at optimal conditions. The obtained results are in excellent accordance with those which are determined by the mathematical modelling of the potentiodynamic polarization curves recorded around OCP (Table 2).

4. Conclusion

The influence of SEBS ratio, immersion 1, and immersion 2 on the corrosion rate of SEBS coated copper in 3 wt % NaCl solution was evaluated by voltammetry around OCP after applying experimental design procedures. The results demonstrated that the SEBS ratio is the most significant parameter that influenced the CR of SEBS coated copper. Besides, even though the immersion 2, the quadratic effect of the SEBS ratio, the immersion 1 and the interaction SEBS ratio—immersion 2 are important, they are less significant. The fit of the experimental design indicated that the optimum

protocol for the SEBS film's formation by dip-coating the surface to obtain a lower corrosion rate could be found at the SEBS ratio of around 2.17 %, the immersion 1 around 20 min, and the immersion 2 around 21 min. The optimal operating conditions found (Cu-SEBS-Opt Cond) were tested on a real protocol, leading to 0.000174 mm year^{-1} of the corrosion rate. This value is near the value found by the experimental design. SEBS film protects effectively the copper from corrosion in an aqueous NaCl solution, indicating a decline in the accessibility of the aggressive species to the copper surface. The potentiodynamic polarization studies substantiate the SEBS coating acts as a cathodic-type corrosion inhibitor. The inhibition efficiencies obtained from the voltammetry around OCP and electrochemical impedance studies are in excellent agreement.

References

1. Mansouri: H.; Eghbali, B.; Afrand, M. Producing Multi-Layer Composite of Stainless Steel/Aluminum/Copper by Accumulative Roll Bonding (ARB) Process. *Journal of Manufacturing Processes* **2019**, *46*, 298–303.
2. Tang, H.; Sun, J.; Pan, J. Electrochemical and Localized Corrosion Behavior of 316 L SS/Copper/316 L SS Sandwich Composite in Chloride-Containing Environment. *Corrosion Science* **2022**, *209*, 110719.
3. Yabuki, A.; Tanabe, S.; Fathona, I.W. Self-Healing Polymer Coating with the Microfibers of Superabsorbent Polymers Provides Corrosion Inhibition in Carbon Steel. *Surface and Coatings Technology* **2018**, *341*, 71–77.
4. Holden, G.; Legge, N.R. Thermoplastic Elastomers Based on Polystyrene–Polydiene Block Copolymers. *Carl Hanser Verlag, Thermoplastic Elastomers: a Comprehensive Review*, **1987**, 47–65.
5. Li, X.; Huang, K.; Wang, X.; Li, H.; Shen, W.; Zhou, X.; Xu, J.; Wang, X. Effect of Montmorillonite on Morphology, Rheology, and Properties of a Poly [Styrene–(Ethylene-Co-Butylene)–Styrene]/Poly (ε-Caprolactone) Nanocomposite. *Journal of Materials Science* **2018**, *53*, 1191–1203.
6. Majesté, J.-C.; Santamaría, A. Rheology and Viscoelasticity of Multiphase Polymer Systems: Blends and Block Copolymers. *Handbook of multiphase polymer systems* **2011**, 311–357.
7. Drobny, J.G. Handbook of Thermoplastic Elastomers; Elsevier, 2014;
8. Grigorescu, R.M.; Ciuprina, F.; Ghioca, P.; Ghiurea, M.; Iancu, L.; Spurcaciu, B.; Panaitescu, D.M. Mechanical and Dielectric Properties of SEBS Modified by Graphite Inclusion and Composite Interface. *Journal of Physics and Chemistry of Solids* **2016**, *89*, 97–106.
9. Zhang, R.; Huang, K.; Zhu, M.; Chen, G.; Tang, Z.; Li, Y.; Yu, H.; Qiu, B.; Li, X. Corrosion Resistance of Stretchable Electrospun SEBS/PANi Micro-Nano Fiber Membrane. *European Polymer Journal* **2020**, *123*, 109394.
10. Masmoudi, F.; Jedidi, I.; Amor, Y.B.; Masmoudi, M. Corrosion Protection Evaluation of Copper Coated with a Block Copolymer and Block Coploymer/Carbon Black Nanoparticles in 3 Wt% NaCl Solution. *ChemistrySelect* **2023**, *8*, e202202608.
11. Mune, M.A.M.; Minka, S.R.; Mbome, I.L. Response Surface Methodology for Optimisation of Protein Concentratepreparation from Cowpea [Vigna Unguiculata (L.) Walp]. *Food chemistry* **2008**, *110*, 735–741.
12. de Lima, T.G.; Rocha, B.; Braga, A.V.C.; do Lago, D.C.B.; Luna, A.S.; Senna, L.F. Response Surface Modeling and Voltammetric Evaluation of Co-Rich Cu–Co Alloy Coatings Obtained from Glycine Baths. *Surface and Coatings Technology* **2015**, *276*, 606–617.
13. Senna, L.F.; Luna, A.S. Experimental Design and Response Surface Analysis as Available Tools for Statistical Modeling and Optimization of Electrodeposition Processes. In *Electroplating*; IntechOpen, 2012.
14. Do Lago, D.C.B.; De Senna, L.F.; Soares, E.C.S.; Da Silva, L.F.; Fernandes, D.S.; Luna, A.S.; D'elia, E. The Use of Experimental Design for the Study of the Corrosion of Bronze Pretreated with AMT in Artificial Rainwater. *Progress in Organic Coatings* **2013**, *76*, 1289–1295.
15. Chaabani, A.; Aouadi, S.; Souissi, N.; Nóvoa, X.R. Electro-Chemical Impedance Spectral (EIS) Study of Patinated Bronze Corrosion in Sulfate Media: Experimental Design Approach. *Journal of Materials Science and Chemical Engineering* **2017**, *5*, 44–54.
16. Rios, E.C.; Zimer, A.M.; Mendes, P.C.; Freitas, M.B.; de Castro, E.V.; Mascaro, L.H.; Pereira, E.C. Corrosion of AISI 1020 Steel in Crude Oil Studied by the Electrochemical Noise Measurements. *Fuel* **2015**, *150*, 325–333.
17. Masmoudi, M.; Assoul, M.; Wery, M.; Abdelhedi, R.; El Halouani, F.; Monteil, G. Wear Behaviour of Nitric Acid Passivated Cp Ti and Ti6Al4V. *Journal of alloys and compounds* **2009**, *478*, 726–730.
18. Masmoudi, M.; Capek, D.; Abdelhedi, R.; El Halouani, F.; Wery, M. Application of Surface Response Analysis to the Optimisation of Nitric Passivation of Cp Titanium and Ti6Al4V. *Surface and Coatings Technology* **2006**, *200*, 6651–6658.
19. Şenaras, A.E. Parameter Optimization Using the Surface Response Technique in Automated Guided Vehicles. In *Sustainable Engineering Products and Manufacturing Technologies*; Elsevier, 2019; pp. 187–197.

20. Masmoudi, M.; Rahal, C.; Abdelhedi, R.; Khitouni, M.; Bouaziz, M. Inhibitive Action of Stored Olive Mill Wastewater (OMW) on the Corrosion of Copper in a NaCl Solution. *RSC advances* **2015**, *5*, 101768–101775.
21. Rahal, C.; Masmoudi, M.; Abdelhedi, R.; Sabot, R.; Jeannin, M.; Bouaziz, M.; Refait, P. Olive Leaf Extract as Natural Corrosion Inhibitor for Pure Copper in 0.5 M NaCl Solution: A Study by Voltammetry around OCP. *Journal of Electroanalytical Chemistry* **2016**, *769*, 53–61.
22. Refait, P.; Rahal, C.; Masmoudi, M. Corrosion Inhibition of Copper in 0.5 M NaCl Solutions by Aqueous and Hydrolysis Acid Extracts of Olive Leaf. *Journal of Electroanalytical Chemistry* **2020**, *859*, 113834.
23. Dhouibi, I.; Masmoudi, F.; Bouaziz, M.; Masmoudi, M. A Study of the Anti-Corrosive Effects of Essential Oils of Rosemary and Myrtle for Copper Corrosion in Chloride Media. *Arabian Journal of Chemistry* **2021**, *14*, 102961.
24. Raza, M.A.; Rehman, Z.U.; Ghauri, F.A. Corrosion Study of Silane-Functionalized Graphene Oxide Coatings on Copper. *Thin Solid Films* **2018**, *663*, 93–99.
25. Yu, Y.; Yang, D.; Zhang, D.; Wang, Y.; Gao, L. Anti-Corrosion Film Formed on HAl77-2 Copper Alloy Surface by Aliphatic Polyamine in 3 Wt.% NaCl Solution. *Applied Surface Science* **2017**, *392*, 768–776.
26. Sui, W.; Zhao, W.; Zhang, X.; Peng, S.; Zeng, Z.; Xue, Q. Comparative Anti-Corrosion Properties of Alkylthiols SAMs and Mercapto Functional Silica Sol–Gel Coatings on Copper Surface in Sodium Chloride Solution. *Journal of Sol-Gel Science and Technology* **2016**, *80*, 567–578.
27. Rahal, C.; Masmoudi, M.; Abdelhedi, R.; Sabot, R.; Jeannin, M.; Bouaziz, M.; Refait, P. Olive Leaf Extract as Natural Corrosion Inhibitor for Pure Copper in 0.5 M NaCl Solution: A Study by Voltammetry around OCP. *Journal of Electroanalytical Chemistry* **2016**, *769*, 53–61.
28. Ghelichkhah, Z.; Sharifi-Asl, S.; Farhadi, K.; Banisaied, S.; Ahmadi, S.; Macdonald, D.D. L-Cysteine/Polydopamine Nanoparticle-Coatings for Copper Corrosion Protection. *Corrosion Science* **2015**, *91*, 129–139.